

# MELANOSOME TRACKING BY BAYES THEOREM AND ESTIMATION OF MOVABLE REGION

Toshiaki Okabe and Kazuhiro Hotta

*Meijo University, 1-501 shiogamaguchi, Tenpaku-ku, Nagoyasi, 468-8501, Japan*

**Keywords:** Tracking, Intracellular image, Melanosome, Systems biology.

**Abstract:** This paper proposes a melanosome tracking method using Bayes theorem and estimation of movable region of melanosome candidates. Melanosomes in intracellular images are tracked manually now to investigate the cause of disease, and automatic tracking method is desired. Since there are little automatic recognition methods for intracellular images, we can not know which features and classifiers are effective for them. Thus, we try to develop the melanosome tracking using Bayes theorem of melanosome candidates detected by Scale-Invariant Feature Transform (SIFT). However, SIFT can not detect the center of melanosome because melanosome is too small in images. Therefore, SIFT detector is adopted after image size is enlarged by Lanczos resampling. However, there are still many melanosome candidates. Thus, we estimate the movable region of the target melanosome in next frame and eliminate melanosome candidates. After the posterior probability of each candidate is computed by Bayes theorem, and the melanosome with the maximum probability is tracked. Experimental results using the melanosome images of normal and Griscelli syndrome show the effectiveness of our method.

## 1 INTRODUCTION

Live cell imaging is advanced rapidly in recent years because of the progress of microscope techniques (Sakaushi et al., 2007; Sugimoto and Tone, 2010; Sakaushi, et al., 2008). Especially, elucidation of transportation path in cells is very important for understanding of clinical state. However, there are little automatic recognition methods for live cell imaging, and human counts and tracks the particles in cells manually now. This work is hard physically and mentally for humans, and human can not treat a lot of data. Since many objective data are required for the investigation into the cause of disease, automatic recognition methods for intracellular images are desired. Therefore, we try to develop a tracking method for intracellular images. This is new application of computer vision and very contributes to medical development.

In this paper, the tracking target is the melanosome in the melanocytes (Kuroda, et al., 2003) (Kuroda, et al., 2004). The melanocyte combines the melanin pigment and stores in cell membrane which is called melanosome. The melanosome is transported into cells. It is known

that transport disorder causes abnormal pigmentation. Thus, the melanosome tracking is important for the investigation into the cause of disease. Figure 1 shows the examples of melanosome images in which melanosome is the particle with black color. We must track a particle which is not different from neighboring particles. If we can realize an automatic melanosome tracking method, it will be applicable to particle tracking in various kinds of cells.

There is a software which is usually used in cell biology. That is called SpotTracker2D which is plugin of imageJ. We try to track melanosome by using the SpotTracker2D but it can not track melanosome well. There are not any conventional studies about automatic melanosome tracking by computer. we can not know which features and classifiers are effective for melanosome tracking. Since we do not have any clues, we divide the melanosome tracking into 2 tasks. The first task is the candidate detection. The second task is the posterior probability estimation of the candidates.

In the first task, we try to detect the melanosome candidates by SIFT (Lowe, 2004). However, SIFT can not detect the center of melanosome because melanosome is too small in the original microscope images. Therefore, SIFT is adopted after original

microscope images are enlarged by Lanczos resampling (Duchon, 1979) (Turkowski and Gabriel, 1990). However, SIFT also detects the characteristic points on non-melanosome by image enlargement. This may induce tracking failures. Thus, we must eliminate the candidates. Thus, the movable region of a tracking target in the next frame is estimated under the assumption that the target melanosome does not pass through other melanosomes.

In the second task, the posterior probability of every candidate which is selected by upper steps is computed by Bayes theorem, and the candidate with maximum probability is tracked. However, SIFT detects some features on the same position. Therefore, the posterior probabilities of all features on the same position are computed independently, and the posterior probabilities on the same position are integrated by sum or product.

The melanosome images of normal and Griscelli syndrome are used in experiments. The accuracy achieves 94.4% when the position of melanosome at time  $t+1$  is predicted from that at time  $t$ . The image enlargement by Lanczos resampling, the estimation of movable region and sum of the posterior probability are effective for this task. Although the accuracy decreases in the task that the correct position of melanosome in only the first frame is given and the positions in the remaining frames are predicted, the possibility of our method is demonstrated by experiments.

This paper is constructed as follows. In section 2, the details of the proposed method are explained. Experimental results are shown in section 3. Finally, conclusions and future works are described in section 4.

## 2 PROPOSED METHOD

Figure 2 shows the flowchart of the proposed method. Candidates detection and feature of candidates are required for melanosome tracking. However, recognition techniques for intracellular images are not established and conventional methods do not exist! Thus, in this paper, we use characteristic feature point detection and descriptor by SIFT. However, feature points are not detected at the center of melanosome because the melanosome is too small in the original microscope images. Therefore, the image size is enlarged by Lanczos resampling, and SIFT is applied to the image enlarged 9 times (Okabe and Hotta, 2011). However, SIFT also detects the feature points on non-melanosomes. Thus,

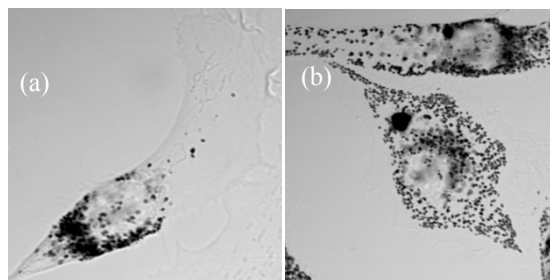


Figure 1: (a) Intracellular image of normal melanocyte (b) Intracellular image of Griscelli syndrome melanocyte.

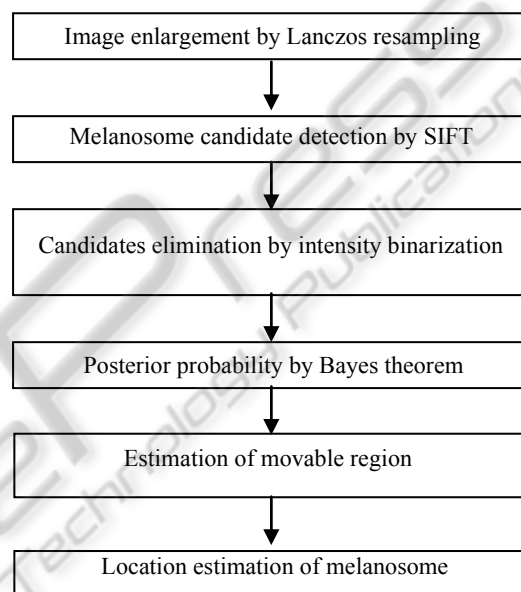


Figure 2: Flowchart proposed method.

melanosome candidates are eliminated by binarization of intensity because the color of melanosome is black. In addition, we estimate the movable region of target melanosome in the next frame under the assumption that the target melanosome does not pass through other melanosomes. The posterior probability of remaining candidates are computed by Bayes theorem, and the position  $\mathbf{x}_t$  with maximum posterior probability is tracked (Okabe and Hotta, 2010). Each element in the proposed method is explained in the following sections.

### 2.1 Scale-Invariant Feature Transform

SIFT is an algorithm for detecting characteristic feature points and for describing the detect points. The characteristic feature points are robust to rotation, scaling and brightness change. Melanosome candidates are detected by SIFT, and SIFT

descriptor is used as the feature for computing the probability.

## 2.2 Image Enlargement by Lanczos Resampling

Since, melanosomes in images are very small, SIFT can not detect correct position. Therefore, image enlargement by Lanczos resampling used to detect correct position of melanosomes.

Lanczos kernel is constructed by the product of 2 sinc functions.

$$L(x) = \begin{cases} \text{sinc}(x)\text{sinc}\left(\frac{x}{a}\right) & -a < x < a, x \neq 0 \\ 1 & x = 0 \\ 0 & \text{otherwise} \end{cases} \quad (1)$$

Sinc function is defined as  $\frac{\sin(\pi x)}{\pi x}$ . The value of "a" is usually set to 2 or 3. When "a" is bigger than the absolute value,  $L(x) = 0$ . When  $x=0$ ,  $L(x)=1$  [15]. Equation (1) can be redefined as

$$\text{sinc}(x)\text{sinc}\left(\frac{x}{a}\right) = \frac{a \sin(\pi x) \sin\left(\frac{\pi x}{a}\right)}{\pi^2 x^2}. \quad (2)$$

The 2 dimensional Lanczos kernel can be made by the product of 1 dimensional kernel. The enlarged image  $\hat{I}(x_0, y_0)$  is computed as

$$\hat{I}(x_0, y_0) = \sum_{i=x_0-a}^{x_0+a} \sum_{j=y_0-a}^{y_0+a} I(i, j) L(x_0 - i) L(y_0 - j). \quad (3)$$

Since Lanczos kernel of  $a=3$  gives clear image enlargement, we use  $a = 3$  in experiments.

## 2.3 Candidates Elimination by Intensity Binarization

SIFT can detect the center of melanosome by image enlargement. However, SIFT also detects non-melanosome regions as shown in Figure 3 (c). Since the color of melanosome is black, non-melanosome candidates with white color are eliminated by intensity binarization. The elimination of candidates will improve tracking accuracy.

When threshold is  $\theta$ , binarization result  $g(x, y)$  is defined as

$$g(x, y) = \begin{cases} 1 & f(x, y) \geq \theta \\ 0 & f(x, y) \leq \theta \end{cases} \quad (4)$$

This threshold value affects tracking accuracy. Therefore, we determine the threshold value experimentally. We evaluate the tracking accuracy for 12 melanosomes for parameter estimation by change the threshold value. Note that these 12

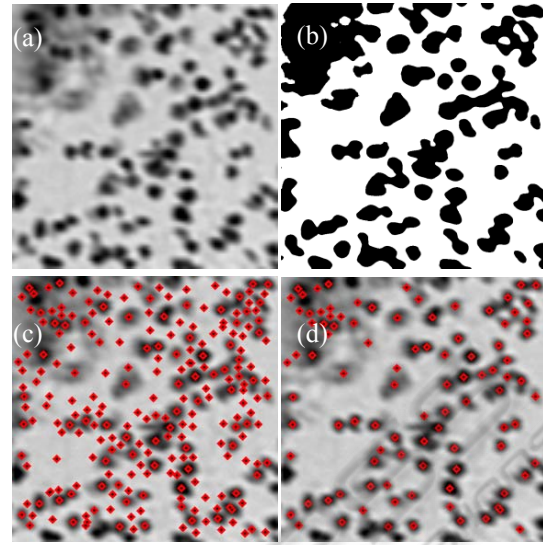


Figure 3: (a) Intracellular image (b) Result of intensity binarization (c) Feature points detected by SIFT are shown as diamond shape (d) SIFT feature points after intensity binarization.

melanosome are not used in test. We found that  $\theta = 100$  gives the best accuracy, and  $\theta$  is set to 100 in the following experiments. Figure 3 (b) is the example of binarization result. Figure 3 (c) is the result of SIFT detector in terms of the image before candidates elimination. On the other hand, Figure 3 (d) shows the result of SIFT detector after candidates elimination. We understand that non-melanosome candidates with white color are eliminated in Figure 3 (d).

## 2.4 Location Prediction by Bayes Theorem

Next we explain there to compute the posterior probability of each candidates. SIFT descriptor with 128 dimensions obtained at the characteristic point  $\mathbf{x}_t$  is used as the feature  $\mathbf{y}_t$  for computing the posterior probability of  $\mathbf{x}_t$ . Since we treat the tracking problem, the posterior probability in terms of  $\mathbf{Y}_t = \mathbf{y}_1, \dots, \mathbf{y}_t$  is considered. Posterior probability  $P(\mathbf{x}_t | \mathbf{Y}_t)$  is computed as

$$P(\mathbf{x}_t | \mathbf{Y}_t) = \frac{p(\mathbf{y}_t | \mathbf{x}_t, \mathbf{Y}_{t-1}) p(\mathbf{x}_t | \mathbf{Y}_{t-1})}{p(\mathbf{y}_t | \mathbf{Y}_{t-1})}. \quad (5)$$

We assume that  $\mathbf{y}_t$  is independent of  $\mathbf{y}_1, \dots, \mathbf{y}_{t-2}$ . Thus,  $p(\mathbf{y}_t | \mathbf{x}_t, \mathbf{Y}_{t-1})$  can be written as  $p(\mathbf{y}_t | \mathbf{x}_t, \mathbf{y}_{t-1})$   $p(\mathbf{x}_t | \mathbf{Y}_{t-1})$  can be written by using the posterior probability at time  $t-1$  and transition probability as

$$p(\mathbf{x}_t | \mathbf{Y}_{t-1}) = \int p(\mathbf{x}_t | \mathbf{x}_{t-1}) p(\mathbf{x}_{t-1} | \mathbf{Y}_{t-1}) d\mathbf{x}_{t-1}. \quad (6)$$

Then, the posterior probability  $P(\mathbf{x}_t | \mathbf{Y}_t)$  can be

written as

$$P(\mathbf{x}_t | \mathbf{Y}_t) = \frac{p(\mathbf{y}_t | \mathbf{x}_t, \mathbf{y}_{t-1}) \int p(\mathbf{x}_t | \mathbf{x}_{t-1}) p(\mathbf{x}_{t-1} | \mathbf{Y}_{t-1}) d\mathbf{x}_{t-1}}{p(\mathbf{y}_t | \mathbf{Y}_{t-1})}. \quad (7)$$

We compute the posterior probability of all candidates and track the location with maximum probability. We do not need to compute  $p(\mathbf{y}_t | \mathbf{Y}_{t-1})$  because it is normalization coefficient.

Conditional probability and transition probability are explained in the following sections.

#### 2.4.1 Conditional Probability

The features of the same melanosome between time  $t$  and  $t-1$  are not so changed. Thus, conditional probability is modelled as normal distribution using the SIFT features at time  $t$  and  $t-1$  as

$$p(\mathbf{y}_t | \mathbf{x}_t, \mathbf{y}_{t-1}) = \frac{1}{\sqrt{2\pi}\sigma} \exp\left\{-\frac{\|\mathbf{y}_t - \mathbf{y}_{t-1}\|^2}{2\sigma^2}\right\}, \quad (8)$$

Where  $\mathbf{y}_t$  is 128 dimensional SIFT descriptor on location  $\mathbf{x}_t$  at time  $t$  and  $\mathbf{y}_{t-1}$  is SIFT descriptor at time  $t-1$ .

#### 2.4.2 Transition Probability

The location of tracking target at time  $t$  and  $t-1$  is denoted as  $\mathbf{x}_t = (w_t, h_t)^T$  and  $\mathbf{x}_{t-1} = (w_{t-1}, h_{t-1})^T$ . If we assume that the melanosome does not move so far from time  $t-1$  to  $t$ , transition probability is also modelled by the normal distribution as

$$p(\mathbf{x}_t | \mathbf{x}_{t-1}) = \frac{1}{\sqrt{2\pi}\sigma} \exp\left\{-\frac{\sqrt{(w_t - w_{t-1})^2 + (h_t - h_{t-1})^2}}{2\sigma^2}\right\}, \quad (9)$$

Equation (9) limits the movable region because transition probability becomes small for far points from  $\mathbf{x}_{t-1}$ .

#### 2.5 Estimation of Movable Region

Figure 3(a) shows that there are many melanosomes with similar appearance in a local region. This

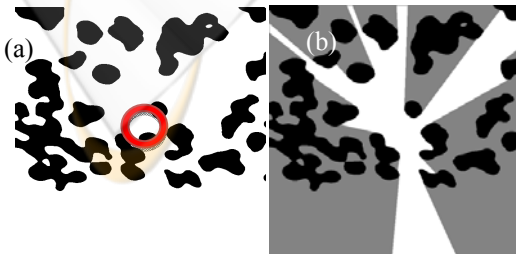


Figure 4: (a) Intracellular image after intensity binarization (b) Movable region of tracking target shown as the red circle in Figure 4(a).

induces tracking failure. The similarity measure by SIFT may not be sufficient. Thus, we estimate the movable region of a tracking melanosome in next frame to improve the accuracy. If we assume that other melanosomes except for the tracking target do not move, we can estimate the movable region of the target. First, we binarize the image as shown in Figure 4(a). Melanosome is represented as black color and the non-melanosome region is represented as white color. The target melanosome is shown as red circle. If target melanosome does not pass through other melanosomes and other melanosomes do not move, we can estimate the movable region as shown in Figure 4(b). The white regions are the movable region in the next frame. Experimental results show that the estimation of movable region decreases the tracking failure.

### 3 EXPERIMENTS

We use the melanosome images obtained from Technical Committee on Industrial Application of Image Processing (<http://www.tc-iaip.org/algorithm.html>). The correct positions of melanosomes in these images are also included. The 44 melanosomes (31 normal and 13 Griscelli syndrome) are used in evaluation. Note that these melanosomes are different from the melanosome used for parameter selection. We evaluate our method in 2 kinds of tasks. The first task evaluates whether the true position of melanosome at time  $t$  is estimated from the supervised position at time  $t-1$ . The second task evaluates whether the position of melanosome at time  $t$  is estimated when the supervised position in only the first frame is given. In the second task, we use the simplest case of our method in which only the posterior probability of tracked position at time  $t-1$  is 1 and that of other positions is 0 because the computational cost and memory requirement are large when the posterior probabilities of all candidates are saved. This corresponds to the case that the method used in the first task is adopted continuously without the supervised position in the previous frame.

In this experiment, we our method is compared with SpotTracker2D which is usually used in cell biology and our proposed method without estimation movable region. SpotTracker2D is a robust tracker for microscope images (Sage et al., 2005). In SpotTracker, LoG filter is used to enhance the target and to reduce noises. After that, target particle is tracked by using dynamic programming. Table 1 shows the accuracy in the first task. Tracking

accuracy of our method is much better than SpotTracker2D. We found that conventional SpotTracker2D is not useful for the melanosome tracking and our method using Bayes theorem and SIFT is effective. Table 2 shows the result of our method with estimation of movable region. Tracking accuracy is improved by estimation of movable region. This shows the effectiveness of the estimation of movable region. Tables also show that sum of probability is better than product. It is known that the integration by sum is effective for several tasks (Kittler et al., 1998) (Hotta, 2009). The best accuracy our method achieves 94.4%. Though SpotTracker2D achieves 73.7%.

In the second task, we do not evaluate SpotTracker2D because it was much lower than the proposed method in the first task. Table 3 and 4 show the result of the second task of our method. Table 3 and 4 show that tracking accuracy for Griscelli syndrome decreases by using our movable region. This is because we assume that another melanosomes except for the tracking target do not move and melanosomes in Griscelli syndrome move actively. Thus, tracking accuracy of Griscelli syndrome decreased slightly. However, the tracking accuracy of Normal melanosome with estimation of movable region is better than that without estimation of movable region. The average of tracking accuracy is improved.

The accuracy in the second task decreased in comparison with the first task. This is because one tracking failure induces the failures in the following frames. We can consider two reasons for inducing one tracking failure. The first reason is SIFT detector. There were some cases that SIFT failed to detect the target melanosome. The proposed method can not track the target when the target melanosome is not detected as the melanosome candidates. In the first task, this failure decreases the accuracy slightly. However, this failure decreases accuracy much more in the second task because the proposed method does not have the obvious function for recovering from the error.

The second reason is the candidate elimination by intensity binarization. In this paper, threshold value is determined as 100 which gives maximum tracking

Table 1: Result in the first task without estimation of movable region.

	Product	Sum	Spot Tracker2D
Griscelli syndrome	91.4%	91.7%	54.6%
Normal	94.6%	94.6%	81.7%
Total average	93.7%	93.8%	73.7%

Table 2: Result in the first task with estimation of movable region.

	Product	Sum
Griscelli syndrome	92.2	92.9
Normal	95.0	95.0
Total average	94.2	94.4

Table 3: Result in the second task without estimation of movable region.

	Product	Sum
Griscelli syndrome	68.2	70.7
Normal	73.4	73.4
Total average	71.9	72.6

Table 4: Result in the second task with estimation of movable region.

	Product	Sum
Griscelli syndrome	66.3	66.5
Normal	78.4	78.4
Total average	74.8	74.9

accuracy in terms of the image set for parameter estimation. However, this threshold may not be appropriate for the test set. Some correct melanosomes were eliminated by intensity binarization. Thus, one failure induced by elimination of candidate decreases the accuracy in the second task. The addition of recovering function from one failure is the future subject. Although the accuracy decreases in the second task, the accuracy achieves 74.9% from only correct position in the first frame. As you understand from Figure 1, our there are many similar objects in local region, and the melanosome is not easy task. The accuracy demonstrates the effectiveness of the proposed method.

## 4 CONCLUSIONS

We proposed a melanosome tracking method using Bayes theorem and estimation of movable region. Since SIFT did not work well for the original images, characteristic feature points are detected after image enlargement. To improve the accuracy, candidates are eliminated by intensity binarization and estimation of movable region. In the first task in which the position at time  $t$  is predicted from the supervised position at time  $t-1$ , the accuracy achieved 94.9%. This is much better than SpotTracker2D which is usually used in cell biology. This shows the effectiveness of our method. However, in the second task in which melanosome is tracked in remaining frames from the supervised

position in only the first frame, one failure induced the error in remaining frames, and the accuracy decreased. However, the accuracy achieved 74.9% for the difficult task in which there are many similar objects around the tracking target. This demonstrates the effectiveness of our method for new and important problem in which conventional methods are little. This paper will be a giant step for intracellular image processing.

The future work is to add a recovering function from tracking failures. We will try the validation from  $t$  to  $t-1$  as well as the position prediction from  $t-1$  to  $t$ .

## ACKNOWLEDGEMENTS

We would like to thank Professor Mitunari Fukuda at Tohoku University and The Japan Society for Precision Engineering and Technical Committee for Industrial Application of Image Processing for providing the opportunity to use melanosome images. This work was supported by KAKENHI (23113727).

## REFERENCES

- T. S. Kuroda, et al., "The actin-binding domain of Slac2-a/melanophilin is required for melanosome distribution in melanocytes", *Mol. Cell. Biol.* 23, pp. 5245-5255, (2003).
- T. S. Kuroda, et al., "Rab27A-binding protein Slp2-a is required for peripheral melanosome distribution and elongated cell shape in melanocytes", *Nature Cell Biol.* 6, pp. 1195-1203, (2004).
- D. G. Lowe, "Distinctive image features from scale-invariant keypoints", *International Journal of Computer Vision*, 60, 2, pp. 91-110, (2004).
- C. E. Duchon, "Lanczos Filtering in One and Two Dimensions", *Journal of Applied Meteorology* 18, 8, pp. 1016-1022, (1979).
- K. Turkowski and S. Gabriel, "Filters for Common Resampling Tasks", In Andrew S. Glassner. *Graphics Gems I. Academic Press*, pp. 147-165, (1990).
- R. O. Duda, et al., Pattern Classification, *JOHN WILEY & SONS*, (2001).
- A. I. Dale, Most Honourable Remembrance: The Life and Work of Thomas Bayes, *Springer*, (1991).
- S. M. Stigler, "Thomas Bayes' Bayesian Inference", *Journal of the Royal Statistical Society, Series A*, 145, pp. 250-258, (1982).
- T. Okabe, K. Hotta, "Tracking of Melanosome is Using Bayes Theorem and SIFT Detector", *MIRU 2010 Satellite workshop on Intracellular image processing* pp. 12, (2010). (in Japanese, without review).
- T. Okabe, K. Hotta, "Accuracy improvement of Melanosome by Image Enlargement", *IEICE General Conference*, Student poster session, (2011) (in Japanese, without review).
- S. Sakaushi, et al, "Dynamic behavior of FCHO1 revealed by live-cell imaging microscopy: it's possible involvement in clathrin-coated vesicleformation", *BiosciBiotechnolBiochem*, 71, 7, pp. 1764-1768, (2007).
- K. Sugimoto and S. Tone, "Imaging of mitotic cell division and apoptotic intra-nuclear processes in multicolor", *Methods Mol. Biol.* 591, pp. 135-146, (2010).
- S. Sakaushi, et al, "Visualization of aberrant perinuclear microtubule asterorganization by microtubule-destabilizing agents", *Cell Cycle.* 7, 4, pp. 477-483, (2008).
- <http://www.tc-iaip.org/algorithm.html>.
- J. Lund and K. L. Bowers, Sinc Methods for Quadrature and Differential Equations, *SIAM*, (1992).
- J. Kittler, M. Hatef, R. Dine and J. Matas, "Combing Classifiers", *IEEE Trans. on Pattern Analysis and Machine Intelligence*, 20, 3, pp. 226-239, (1998).
- K. Hotta, "Pose Independent Object Classification from Small Number of Training Samples Based on Kernel Principal Component Analysis of Local Parts", *Image and Vision Computing*, 27, pp. 1240-1251, (2009).
- D. Sage, et al, "Automatic Tracking of Individual Fluorescence Particles: Application to the Study of Chromosome Dynamics," *IEEE Transactions on Image Processing*, 14, 9, pp. 1372-1383, (2005).